Air-Water Interfacial Collapse and Rate-Limited Solid Desorption Control Perfluoroalkyl Acid Leaching from the Vadose Zone

John F. Stults,[a*] *Charles E. Schaefer,*[a,b] *Yida Fang,*[a,c] *Julie Devon,*[a] *Dung Nguyen,*[a] *Isreq Real,*[d] *Shilai Hao,*[e] *Jennifer L. Guelfo*[d]

[a]CDM Smith, 14432 SE Eastgate Way, Suite 100, Bellevue, WA 98007, United States

[b]CDM Smith, 110 Fieldcrest Avenue, #8, 6th Floor, Edison, New Jersey 08837, United States

[c]Haley and Aldrich Inc., 3131 Elliott Ave #600, Seattle, WA 98121

[d]Civil, Environmental, and Construction Engineering, Texas Tech University, Lubbock, TX 79409, USA

[e]Civil & Environmental Engineering, Colorado School of Mines, Golden, CO 80401, USA

* Corresponding author's contact info: Tel.: (303) 815-8730; E-mail: stultsjf@cdmsmith.com

Abstract

Some Per- and polyfluoroalkyl substances (PFAS) are strongly retained in the vadose zone due to their sorption to both soils and air-water interfaces. While significant research has been dedicated to understanding equilibrium behavior for these multi-phase retention processes, leaching and desorption from aqueous film-forming foam (AFFF) impacted soils under field relevant conditions can exhibit significant deviations from equilibrium. Herein, laboratory column studies using field collected AFFF-impacted soils were employed to examine the leaching of perfluoroalkyl acids (PFAAs) under simulated rainfall conditions. The HYDRUS 1-D model was calibrated to estimate the unsaturated hydraulic properties of the soil in a layered system using multiple boundary condtions. Forward simulations of equilibrium PFAS partitioning using the HYDRUS model and simplified mass balance calculations showed good agreement with the net PFAS mass flux out of the column. However, neither were able to predict the PFAS concentrations in the leached porewater. To better understand the mechanisms controlling the leaching behavior, the HYDRUS 1-D two-site leaching model incorporating solid phase rate limitation and equilibrium air-water interfacial partitioning was employed. Three variations of the novel model incorporating different forms of equilibrium air-water interfacial partitioning were considered using built-in numerical inversion. Results of numerical inversion show that a combination of air-water interfacial collapse and rate-limited desorption from soils can better predict the unique leaching behavior exhibited by PFAAs in AFFF-impacted soils. A sensitivity analysis of the initial conditions and rate-limited desorption terms was conducted to assess the agreement of the model with measured data. The models demonstrated herein show that, under some circumstances, laboratory equilibrium partitioning data can provide a reasonable estimation of total mass leaching, but fail to account for the significant rate-limited, non-Fickian transport which affect PFAA leaching to groundwater in unsaturated soils.

Introduction

Per- and poly-fluoroalkyl substances (PFAS) are a large class of chemicals with low criteria for toxicity calculated from risk based approaches which are recalcitrant within the environment (Fenton et al., 2021; Guelfo et al., 2021; Sharifan et al., 2021; Sima and Jaffé, 2021). PFAS high potential for bioaccumulation, low criteria for toxicity, and pervasive environmental occurrence compound the issue of their environmental challenges (Anderson et al., 2016; Brusseau et al., 2020; Guelfo and Adamson, 2018). Soil and groundwater are typically impacted by PFAS due to release of aqueous film-forming foams (AFFFs) (Anderson et al., 2016; Moody and Field, 1999), waste disposal (Lang et al., 2017), wastewater treatment plant effluent (Islam et al., 2023), aerosol deposition (Faust, 2023; Johansson et al., 2019), and numerous manufacturing processes (Glüge et al., 2020). Currently, *in situ* treatment technologies are not commercially available and fully validated for PFAS, while *ex situ* soil treatments are relatively expensive and not readily available (Ross et al., 2018). Thus, proper assessment of PFAS fate and transport, particularly in AFFF-impacted soil source areas, is critical to properly determine the extent to which source area treatment is needed.

PFAS commonly enter subsurface systems during surface applications and must migrate through the vadose zone prior to entering groundwater systems (Anderson et al., 2016; Brusseau et al., 2020; Faust, 2023). PFAS transport within the vadose is coupled to the water flux, but is subject to other physiochemical processes (i.e. adsorption to surfaces and transformation) which can influence transport behavior (Brusseau and Rao, 1989; Šimůnek and Genuchten, 2008). Reactive transport models which treat PFAS transport as a Fickian equilibrium process have asserted that PFAS contamination will persist for centuries without vadose zone remediation (Ruyle et al., 2023). However, transient and heterogenous conditions in the vadose zone

77 frequently produce non-Fickian, reactive transport processes which can have unexpected results
78 (Ben-Noah et al., 2023; Hasan et al., 2020; Zeng and Guo, 2023).

79 There are several models which can quantify the effects of non-Fickian transport and
80 chemical sorption non-equilibrium. The fundamental examples of these models are the two-site
81 adsorption model and the mobile-immobile model (MIM) (van Genuchten and Wagenet, 1989).
82 The two-site adsorption model is less physically robust in its treatment of the non-equilibrium
83 domain but can more easily quantify both non-equilibrium adsorption and the effect of immobile
84 water with less explicit informational inputs. The classical MIM is more physically robust, as it
85 explicitly quantifies the amount of immobile water in the pore space and quantifies a
86 macroscopic mass transfer coefficient of transport from the advective to the diffusion limited
87 domain. At the time of this publication, HYDRUS is the only commercially available software
88 which can quantify both air-water interfacial adsorption of PFAS and rate-limited, non-Fickian
89 transport processes in the vadose zone (Silva et al., 2020).

90 PFAS have several potential retention processes which can vary based on the type of source
91 zone (Brusseau, 2018; Brusseau and Guo, 2022), the hydrophobicity of the PFAS (i.e. potential
92 adsorption to the air-water interface) (Brusseau and Guo, 2022; Stults et al., 2023), and soil
93 properties (Brusseau, 2023a; Wanzek et al., 2023). In general, solid phase and the air-water
94 interfacial partitioning of PFAS are the two retardation and retention mechanisms that are of
95 greatest concern at most field locations (Brusseau, 2018; Brusseau and Guo, 2022; Schaefer et
96 al., 2022a). Equilibrium solid phase adsorption is a complex function of PFAS structural
97 characteristics (e.g., carbon chain length and functional groups), cation/anion exchange capacity,
98 soil pH, total organic carbon (TOC) content, silt/clay content, and specific surface area (SSA)
99 (Knight et al., 2019; Kookana et al., 2022; Nguyen et al., 2020; Umeh et al., 2021; Wanzek et al.,

2023). Currently, there is debate over whether a concentration dependent Freundlich isotherm or a concentration independent Langmuir isotherm is applicable for equilibrium air-water interfacial partitioning of PFAS below a critical reference concentration (CRC) (Arshadi et al., 2020; Brusseau et al., 2021; Schaefer et al., 2020, 2019; Stults et al., 2023, 2022). There are a number of studies and methodologies supporting both the application of a Freundlich (Abraham et al., 2022; Schaefer et al., 2022b, 2022a, 2019; Stults et al., 2023, 2022) and Langmuir (Arshadi et al., 2020; Brusseau et al., 2021; Brusseau and Guo, 2022; Le et al., 2021) isotherms below the CRC, which we detail in a prior publication (Stults et al., 2023). There is also a rapidly evolving understanding of the mechanisms of solid phase adsorption of PFAS (Nguyen et al., 2020). Recent evidence suggests there are non-labile or significantly rate limited fractions of PFAS mass which do not readily desorb from natural soils (Huang et al., 2023; Schaefer et al., 2021; Wanzek et al., 2023). This non-labile mass has been directly quantified for PFAS contamination associated with AFFF applications (Schaefer et al., 2021; Wanzek et al., 2023).

A significant amount of work has been performed evaluating PFAS transport through saturated, PFAS free soil and sandy material which shows solid phase partitioning can be at non-equilibrium (Brusseau et al., 2019; Guelfo et al., 2020; Lyu et al., 2018; Van Glubt et al., 2021; Wang et al., 2021; Zhou et al., 2021) or irreversibly adsorb a large fraction of mass (Wanzek et al., 2023). One study in particular demonstrated that both short and long chain perfluoroalkyl acids (PFAAs) solid partitioning could be better simulated with a two-site non-equilibrium model than with equilibrium models (Guelfo et al., 2020). However, less work has been done to understand the desorption of PFAS from multi-phase vadose zone soils. Experimental studies have shown that solid desorption processes remain poorly understood (Huang et al., 2023; Maizel et al., 2021; Schaefer et al., 2021). Other studies have shown field

behavior of PFAAs often can be reasonably described by equilibrium partitioning (Brusseau, 2023a; Schaefer et al., 2024, 2023). While some transient leaching studies (Høisæter et al., 2019; Schaefer et al., 2023, 2022a) and modelling studies (Wallis et al., 2022; Zeng and Guo, 2023, 2021) have been conducted for PFAS in unsaturated conditions, very little well controlled experimental data exist which could better elucidate the mechanisms of vadose zone PFAS leaching under realistic conditions.

This study attempts to better understand the mechanisms of PFAS desorption from AFFF-impacted soils using well controlled laboratory leaching experiments and modeling with HYDRUS 1-D. An AFFF-impacted soil was collected and characterized prior to this study (Maizel et al., 2021; Schaefer et al., 2023, 2022c, 2021), and was evaluated in a series of transient flow unsaturated column experiments that were designed to simulate PFAS leaching during wetting and drying cycles. HYDRUS 1-D and a cell-based mass balance showed PFAS mass flux could reasonably estimate the total mass flux from the column using equilibrium partitioning parameters. However, equilibrium partitioning could not describe the temporal dynamics of PFAS leaching with respect to the solute concentration in the eluate. It was theorized that rate-limited solid desorption from soils, consideration of labile vs non-labile mass fractions, and equilibrium air-water interfacial partitioning could significantly improve the simulation of PFAA dynamics in the eluate.

Materials & Methods

Experimental Materials & Methods

Column Materials and Packing

Four identical soil leaching columns (two using AFFF-impacted soil, and two using a clean sand) were constructed from 5 cm diameter acrylic (Figures S.1-2). The columns were a

146 total of 17 cm long. A 400x400 stainless steel screen mesh was placed on the base of the column
147 to support the porous material and prevent removal of fines immediately above a small volume
148 water trap. A saturated 3 cm silica flour cake was placed on the bottom to prevent disaggregation
149 of the media (Figures S.1-S.3). The air-entry pressure for the 45μm silica flour was 250 mm Hg
150 from Soil Moisture Corporation (Goleta, California). Prior to column leaching testing using the
151 AFFF impacted soil, control studies were conducted to ensure adsorption of PFAS to the column
152 materials (including the silica flour) was negligible (Figure S.4).
153 Immediately above the silica flour cake, 300 grams (10.2 cm in length) of homogenized
154 AFFF impacted soils or control sand were packed into the column. Soils were homogenized by
155 coning and quartering the samples. The columns were dry packed at 1 cm intervals. Each column
156 material was packed in duplicate for a total of 4 columns (Figures S.2-S.3). Directly above the
157 AFFF-impacted soils, a 65 gram (3 cm length) of 0.3-0.4 mm silica sand was placed to help
158 promote uniform distribution simulated rainfall prior to entering the column. The initial moisture
159 content in the column was determined based on the initial soil moisture content (determined
160 gravimetrically at 13% by volume prior to packing). A synthetic, PFAS-free rainwater was
161 prepared using the recipe shown in Table S.1.
162 *Porous Media*
163 An AFFF-impacted soil was collected from a previously studied, former fire training area
164 in the Northeastern United States (Schaefer et al., 2023, 2021). Total PFAS mass in the soil was
165 determined as noted in the analytical methods section. The media itself was characterized for its
166 physical properties (i.e., grain size distribution, sand/silt/clay ratio) to estimate air-water
167 interfacial scaling factor values (Figure S.5). Chemical properties of the soil (TOC, pH) were
168 analyzed as well (SI.1). A control column using oven dried sand (0.3-0.4 mm diameter - Reco

169 Group) was also prepared to ensure any PFAS leaching from the soil column was not attributable
170 to any of the column materials or synthetic rainwater.
171 *Rainfall Simulation Experiments*
172 A peristaltic pump was calibrated to a flow rate that correlates to the volume of rain
173 needed for each rain event. The peristaltic pump was used to deliver a predetermined amount of
174 rainwater to the top of the column over the interval specified in Table S.2. At the start of each
175 rain event, the peristaltic pump and vacuum (100mm Hg) were turned on for the length of time
176 specified in the rain event schedule (Table S.2). Rain events correspond to light (0.3 inches over
177 3 hours), heavy (0.6 inches over 3 hours), and storm (1 inch over 3 hours) rainfall events
178 observed at the field location. Once no more water could be removed from the column, the
179 vacuum was turned off to prevent over-drying of the column and potentially the silica flour. The
180 length of vacuum application is specified in Tables S.3-4 along with all other boundary
181 conditions required for HYDRUS model input. Before beginning the next day's rain event,
182 additional vacuum was applied for 1 hour to collect any residual leachate that occurred overnight
183 due to residual vacuum in the column. After 1 hour of vacuum, the residual leachate sample was
184 collected, and the experimental setup was reset for the next rain event. The porosity of the soil
185 was measured to be 0.405 via gravimetric mass balance after fully saturating a dry, packed
186 sample. The residual water content was assumed to be 0.045 based on the USDA sandy soil
187 classification. Moisture content was measured at the start of the experiment and for a subset of
188 data during an extended drying period in the 29-50 day range of the experiment. The changes in
189 water content were used to estimate the evaporation rate from the column as detailed in SI.1 and
190 Figure S.6.
191 *Sample Preparation and Analysis*

Prior to analysis, soils were extracted using a previously published method (Shojaei et al., 2022), and aqueous samples were diluted in methanol amended with an internal standard (IS) mixture to achieve a final concentration of 200 ng/L. Analysis of PFAS in aqueous sample and soil extracts was performed on a quadrupole time of flight mass spectrometry (QTOF-MS; X500R, SCIEX, Framingham, MA, USA) coupled to a Sciex Exion AC high performance liquid chromatography system (LC), using previously published methods (Shojaei et al., 2022). Briefly, data were collected using a multiple reaction monitoring high resolution (MRMHR) acquisition mode, and two transitions (quantifier and qualifier) were monitored for each of 26 PFAS monitored (Table S.3), where possible. Sciex OS was used for data acquisition and processing. A minimum of two injections per sample were quantified over a calibration range of 1-5000 ng/L (R^2>0.99) using isotope dilution, and concentrations were reported as the average of duplicate injections. Quality control samples included method blanks, solvent blanks, instrument sensitivity checks, and calibration verification. IS recoveries were used to evaluate extraction efficiency and matrix effects. More details regarding sample preparation, chromatographic and mass spectrometer conditions, and quality assurance quality control are available in SI.2.

Modeling Methods

Numerical models of water flow and PFAS transport were calibrated and validated using HYDRUS 1-D with the PFAS module add-on package. The two-site kinetic model was implemented for the system assuming the equilibrium and non-equilibrium phases were initially at equilibrium for the inversion modelling. An additional forward sensitivity analysis was conducted for PFOS and PFPeS where the equilibrium and non-equilibrium concentrations were initially specified to investigate the effect of rate-limited desorption and equilibrium (*f*) vs. non-equilibrium mass fractions.

Mathematical Modelling – Unsaturated Flow

HYDRUS 1-D utilizes the standard form of Richards equation to calculate water flux and changes in water content through the 1-D domain. Richards equations postulates that changes in water content in unsaturated porous media are a function of the hydraulic conductivity, capillary pressure, and gravitational force of water (Richards, 1931). Equation 1 is Richards Equation and Equation 2 is the Darcy Flux Equation for unsaturated systems.

$$\frac{\partial \theta}{\partial t} = \frac{\partial}{\partial z}\left[K(\psi)\left(1 + \frac{\partial \psi}{\partial z}\right)\right] \qquad \textbf{Equation 1}$$

$$q = -K(\psi)\left(1 + \frac{\partial \psi(\theta)}{\partial z}\right) \qquad \textbf{Equation 2}$$

Where θ is the volumetric water content of the porous media, t is time, z is longitudinal distance along 1-D domain, $K(\psi)$ is the unsaturated hydraulic conductivity of the media, ψ is capillary pressure in units of length, and q is the 1-D Darcy flux.

To utilize Richards Equation and the Darcy Equation, a relationship between volumetric water content, capillary pressure, and the unsaturated hydraulic conductivity must be established. This is more commonly referred to as the water retention function, commonly estimated using the Van Genuchten equation. The Van Genuchten equation is preferable to other solutions because it is a closed form equation that allows for easier convergence of the soil hydraulic parameters determined from numerical inversion. The capillary pressure – water content relationship is presented in Equation 3, while the water content – unsaturated hydraulic conductivity relationship is presented in Equation 4.

$$\frac{\theta - \theta_r}{\theta_s - \theta_r} = \Theta = \left[\frac{1}{1 + (\alpha\psi)^n}\right]^m \qquad \textbf{Equation 3}$$

$$\frac{K(\psi)}{K_s} = \Theta^{0.5}\left[1 - \left(1 - \Theta^{\frac{1}{m}}\right)^m\right]^2 \qquad \textbf{Equation 4}$$

Where θ_r is the residual water content, θ_s is the porosity of the media or saturated water content, α is the capillary pressure scaling term of the Van Genuchten equation, n is the function shaping term of the Van Genuchten Equation, $m = 1 - \left(\frac{1}{n}\right)$, and K_s is the saturated hydraulic conductivity of the media.

The column was simulated as a 16.2 cm long layered system. The top 3 cm layer was a 0.3-0.4 mm silica sand (similar to 40/50 accusand), the 10.2 cm middle layer was the impacted AFFF soil, and the bottom 3 cm layer was the silica flour. The Van Genuchten parameters for the top layer of sand were estimated using a built in neural network in HYDRUS 1-D, and the hydraulic conductivity was assumed to be similar to a 40/50 accusand measured in (Schroth et al., 2001). The Van Genuchten parameters and hydraulic conductivity of the bottom layer of silica flour were assumed to be similar to a clay with high water retention and estimated using the USDA soil classification tool built-in to HYDRUS. The HYDRUS 1-D inversion tool was used to estimate the K_s, α, and n terms most well suited to the AFFF impacted media for this column study as described in the next section. Once these three parameters were determined, the Darcy Flux was used to couple the contaminant transport equation to measurements of water flux. A graphical illustration of the layered system and a table of the assumed parameters are presented in Figure 1.

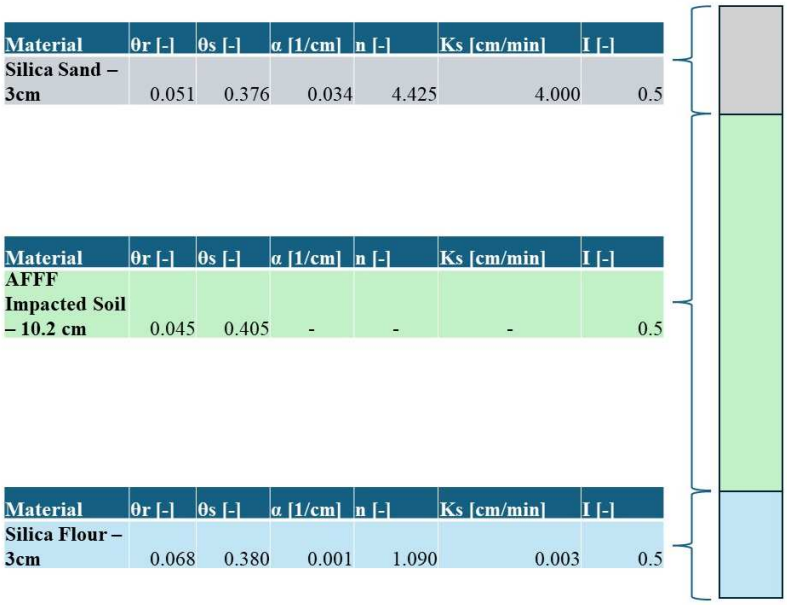

Figure 1: A simplistic graphical representation of the soil column and the parameters used for input to the model. Fields in the table left plant for the AFFF impacted soil are the parameters which are estimated via numerical inversion of the water flux and measured water content data.

The saturated hydraulic conductivity (K_s) and empirical Van Genucthen parameters (α, n) were estimated using measured water flux data and estimated water content data as the objective functions. The top column had an atmospheric boundary condition which allowed for precipitation and evaporation. Precipitation occurred at a constant rate during each simulated 15 storm events. The length and rainfall rate of each event are presented in Table S.2. The evaporation rate was determined experimentally as a function of the days after the last rain event (Figure S.6). Ponding of 0.5 cm of water at the top of the column was allowed, as it was observed that water did not always immediately enter the column. A variable flux boundary condition and variable head boundary condition were simulated for the base of the column to determine which most appropriately simulated changes in measured water content (SI.3). All transient boundary condition inputs for HYDRUS are summarized in Tables S.3 & S.4.

Mathematical Modelling – PFAS Transport

The solute dispersivity in all simulations was assumed to be 0.1 cm for all media, consistent with literature reported values for low dispersion sandy media (Zhuang et al., 2021). Forward, equilibrium simulations of PFAS transport were performed using calibrated water flux data and empirical/estimated equilibrium partitioning data for PFAS. The details of the equilibrium partitioning model are presented in Equations S.1-S.3. A daily mass balance-based calculation (Equation S.6) using the retardation factor from Equation S.1 was performed to serve as a comparison to the HYDRUS model results. More detail on the mass balance model is provided in SI.3.

The two-site kinetic contaminant transport model available in HYDRUS was used in this study due to observation of equilibrium (labile) adsorption sites and very slowly desorbed mass on kinetically limited (non-labile sites) in a previous study (Schaefer et al., 2021). The traditional two-site model has one fraction of equilibrium sites and one fraction of kinetically limited sites. The 1-D transport equation which accounts for labile and non-labile mass fractions as well as air-water interfacial partitioning for each PFAS is presented in Equations 5a-c.

$$\frac{\partial(\theta C_w)}{\partial t} + \rho_b \frac{\partial s_e}{\partial t} + \rho_b \frac{\partial s_k}{\partial t} + \frac{\partial(\Gamma A_{aw})}{\partial t} = \frac{\partial}{\partial x}\left(\theta D_w \frac{\partial C_w}{\partial x}\right) - \frac{\partial(qC_w)}{dx} \quad \textbf{Equation 5a}$$

$$\rho_b \frac{\partial s_k}{\partial t} = \alpha_k \rho_b (C_s - s_k) \quad \textbf{Equation 5b}$$

$$C_s = fK_d C_w + (1-f)K_d C_w = s_e + s_k \quad \textbf{Equation 5c}$$

Where C_w is the aqueous PFAS concentration, ρ_b is the bulk density, S_e is the equilibrium (labile) adsorbed PFAS concentration, S_k is the non-equilibrium (non-labile) adsorbed PFAS concentration, Γ is the surface excess at the air-water interface, A_{aw} is the air-water interfacial area, D_w is the media dispersion term, α_k is the kinetic desorption parameter, and C_s is the

equilibrium solid phase concentration, and f is the fraction of equilibrium adsorption sites. The implementation of the inversion method for this model in HYDRUS is described in SI.4.

Solid phase desorption behavior of this system is assumed to were found to follow a two site kinetic model type behavior under saturated conditions (Schaefer et al., 2022a, 2022c, 2021). Simply, fraction of mass (f) is assumed to be at equilibrium (labile) while the other fraction was found to be at non-equilibrium (non-liabile). The K_d values used in the models were obtained from prior desorption isotherm studies on this soil (Schaefer et al., 2022c). The air-water interfacial area of the soil was estimated using the thermodynamic estimation of air-water interfacial area built in to HYDRUS as shown in Equation S.3 (Silva et al., 2020). However, the thermodynamic estimation of air-water interfacial areas has been previously demonstrated to underpredict air-water interfacial areas (Brusseau and Guo, 2021; Silva et al., 2022). Thus the air-water interfacial scaling term built into HYDRUS was used to correct the air-water interfacial area (Silva et al., 2020). The mean scaling factor for this media was calculated to be 5 using the empirical correlation from (Brusseau, 2023b) presented in Equation 6.

$$A_{aw} = A_{thermo} * (SF_{mean}) = A_{thermo} * [(-0.45 * d_{50}) + 5] \quad \textbf{Equation 6}$$

Where A_{thermo} is the air-water interfacial area predicted by Equation S.3 with a scaling factor of 1, SF_{mean} is the average scaling factor from (Brusseau, 2023b), and d_{50} is the median grain diameter. The d_{50} measured for this media is approximately 0.04 cm (Figure S.5)

PFAS Mechanistic Evaluation Using Numerical Inversion

Initial forward simulations of equilibrium PFAS partitioning were conducted to provide a baseline for assessing PFAS fate and transport. The initial equilibrium simulations assumed linear adsorption the solid phase, and used an estimation of the average K_{ia} based on the mean effluent concentration using the ppQSPR from (Stults et al., 2023). The measured mass flux of

PFAS from the column as well as the measured leachate concentration were compared against simulated data. Based on results from previous studies (Maizel et al., 2021; Schaefer et al., 2021), it is expected that equilibrium modelling will not be sufficient to simulate the desorption behavior of PFAS under simulated rainfall conditions. Initial forward simulation models were performed using the modified version of HYDRUS 1-D (Silva et al., 2020) and a mass balance model (Brusseau and Guo, 2022; Schaefer et al., 2022a) to confirm this finding and serve as a comparative baseline.

For the non-equilibrium inversion models, three different conceptual non-equilibrium models were developed for simulating PFAS fate and transport of PFAS in the columns where all PFAS mass is assumed to be initially in the non-equilibrium domains at the start of the column experiments.

1) Freundlich adsorption to the air-water interface with rate-limited linear partitioning to solid surfaces. (Freundlich AWIA)
2) No air-water interfacial adsorption with rate-limited linear partitioning to solids. (no AWIA)
3) Langmuir (linear below the CRC) adsorption to the air-water interface with rate-limited linear partitioning to the solid surface. (linear AWIA)

Numerical inversions were performed using the PFAS effluent concentration data as the objective function (Jacques et al., 2012; Stults et al., 2022). In all three model inversions, the fraction of equilibrium adsorption sites (*f*) and the rate-limited solid phase desorption coefficients (α_k) were estimated. Model appropriateness was evaluated using the R^2 and Akaike Information criteria (AIC) comparisons. AIC is a common tool used to determine a model likelihood of appropriateness compared to other models. A lower AIC value indicates a higher likelihood of

model appropriateness, which can be more accurately quantified using AIC weights (wAIC) (Wagenmakers and Farrell, 2004).

Results and Discussion

Estimation of Water Flux Parameters

Hydraulic properties of the media were calculated in preparation for equilibrium simulations of the column data for variable flux and variable head boundary conditions. The flux-based boundary conditions (R^2 = 0.995, AIC = -558) significantly outperformed the head-based boundary conditions (R^2 = 0.977, AIC = -491). While neither solution is necessarily unique to the soil, the flux-based boundary condition provides a more accurate simulation of the measured average water content and water flux through the base of the column. The van Genucthen parameters for the soil are presented in Table 1 and fitted vs. observed data are presented in Figure 2a-b.

Table 1: Fitted Van Genuchten Parameters for the AFFF impacted soil column data.

			95% CI	
Variable	**Value**	**S.E.Coeff.**	**Lower**	**Upper**
α [1/cm]	1.32E-01	5.79E-02	1.72E-02	2.47E-01
n [-]	1.85E+00	2.58E-01	1.34E+00	2.36E+00
K_s [cm/min]	5.60E-01	1.99E-01	1.66E-01	9.54E-01

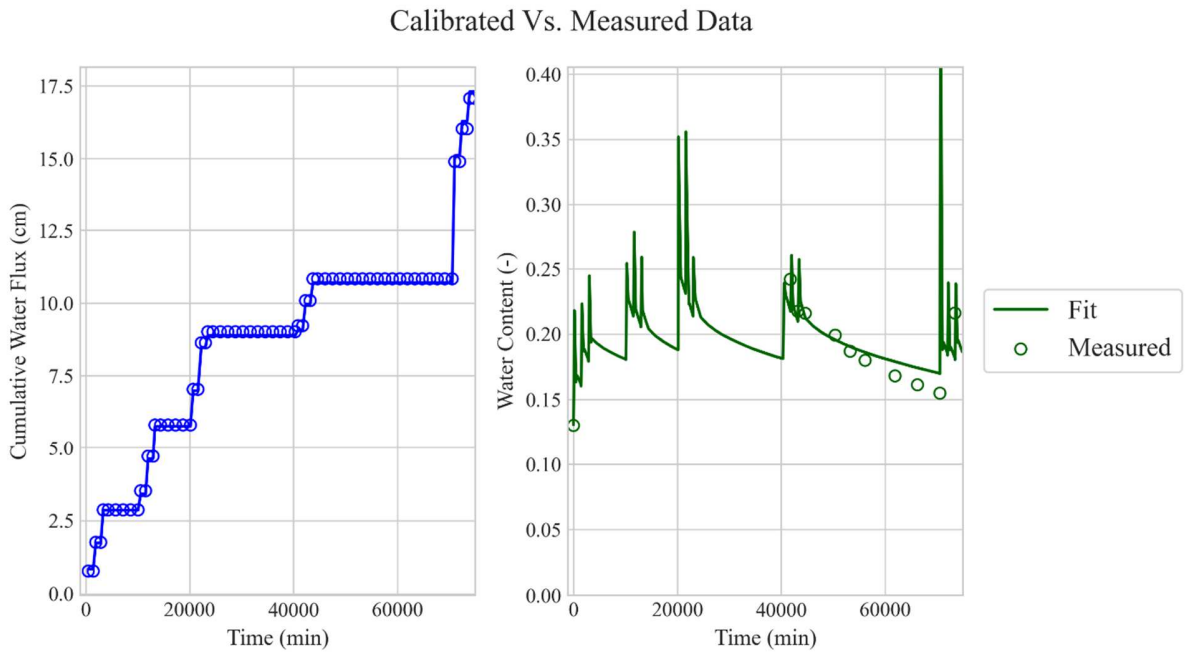

Figure 2a-b: (a – left) The cumulative water flux of measured data vs. the simulated data from the fitted van genuchten parameters. (b – right) average volumetric water content in the column vs. simulated data.

The application of constant flux allowed for a precise calibration of the model to the measured water flux from the experiments. This is of critical importance as multiple studies have identified water flux as a key term controlling PFAS mass flux from the vadose zone to groundwater (Newell et al., 2023; Wallis et al., 2022). Evaporation from the top of the column was not constant with time and followed a decreasing power law correlation. This decreasing evaporation rate with time is in good agreement with measured decreasing evaporation rates from layered sandy systems (Shokri et al., 2010) (Figure S.6). The baseline water content generally increases from 0.13 to around 0.23 during the first 3 rain cycles. The simulated results demonstrate how water typically moves through the sandy system in the form of a large pulse, which dramatically increases both the hydraulic conductivity and decreases the air-water interfacial area of the porous media. This combined effect is expected to produce significant release of PFAS from the soil system. Additional details on the changes in water flux and water

content associated with head based and flux-based models can be found in Figure S.7-9 and the associated text.

Qualitative Assessment of Leaching Data

The six PFAS observed and examined in this study (PFBS, PFPeS, PFHxS, PFOS, PFPeA, and PFOA) are all PFAAs which can be categorized as long chain (PFOS, PFOA) or short chain (PFBS, PFPeS, PFHxS, PFPeA) compounds. These six PFAS were selected because solid phase partitioning to the soil had been sufficiently characterized in a prior study and were observed in the leachate herein (Schaefer et al., 2021; Schaefer et al., 2022c). In general, the two long chain compounds initially had relatively low concentrations in the column effluent over the first 3-day wetting cycles before increasing to a steady state effluent concentration in the second or third 3-day wetting cycle (Figure S.11). Short chain compounds initially spiked to a relatively high effluent concentration during the first wetting cycle and then gradually decreased in concentration over the next four wetting cycles (Figure S.11). This leaching behavior suggested that the short-chain PFAS mass became rapidly depleted in the columns, while the long-chained PFAS had relatively low mass depletion. To confirm this observation, the total mass leached was calculated and plotted against the liquid volume released relative to total solid mass (Figure S.12). Short chain components tended to leach mass more rapidly than longer chain components, consistent with previous observations (Maizel et al., 2021; Schaefer et al., 2023, 2021). Interestingly, the total PFPeA mass leached from the column was over 100% of the total mass measured in the original sample. It is possible that this discrepancy in mass balance was due to precursor transformation, as 6:2 FTS (a known PFPeA precursor) (Yang et al., 2022) was present at concentrations 10x higher than PFPeA (Schaefer et al., 2022c, 2021).

Initial Equilibrium Simulations

The rationale for initial equilibrium simulations is presented in SI.3, with the equilibrium transport equations presented in Equations S.1-S.3. The K_d and labile (equilibrium - *f*) fraction data were obtained from (Schaefer et al., 2022c) and previously unpublished data associated with that work now presented in SI.5, Figure S.10. Air water interfacial partitioning coefficients (K_{ia}) values were obtained from (Stults et al., 2023) using the mean effluent concentration as the input for the concentration term in the poly-parameter quantitative structure property relationship (ppQSPR). No correction was made for ionic strength as the groundwater fell within the typical range of environmental ionic strengths, which would results in a change of less than 15% between 0.001M and 0.1 M Ionic Strength (Stults et al., 2023).

In the initial equilibrium simulations, it assumed that only the labile mass fraction (*f*) is desorbed throughout the course of the experiments. In plain language, the labile mass is assumed to be at equilibrium while the non-labile fraction (1-*f*) is apparently (or, effectively) irreversibly adsorbed to the solid surface (air-water interfacial adsorption is assumed to be reversible and non-hysteretic). In practice PFAS are likely not irreversibly adsorbed, but rather have such slow desorption rates that adsorption appears irreversible over the 52-day experimental period. Results of the porewater concentrations predictions are presented in Figure 3a-b, input data for the equilibrium model is presented in Table 2, and the cumulative mass flux predictions are presented in Figure S.13.

Table 2: The input parameters for the initial Equilibrium HYDRUS models and mass balance calculations

Compound	Initial Mass (ng/g)	Labile Fraction (*f*)	Labile Mass (ng/g)	K_d (cm^3/g)	K_{ia} (cm)
PFBS	25.3	0.26	6.6	5.6	9.44E-04
PFPeS	53.4	0.51	27.2	5.7	2.50E-03
PFHxS	1012.1	0.4	404.8	5.6	3.67E-03
PFOS	2590.2	0.23	595.7	6.9	3.94E-02
PFPeA	3.2	0.71	2.3	1.3	1.23E-03
PFOA	35.2	0.53	18.7	2.2	4.34E-02

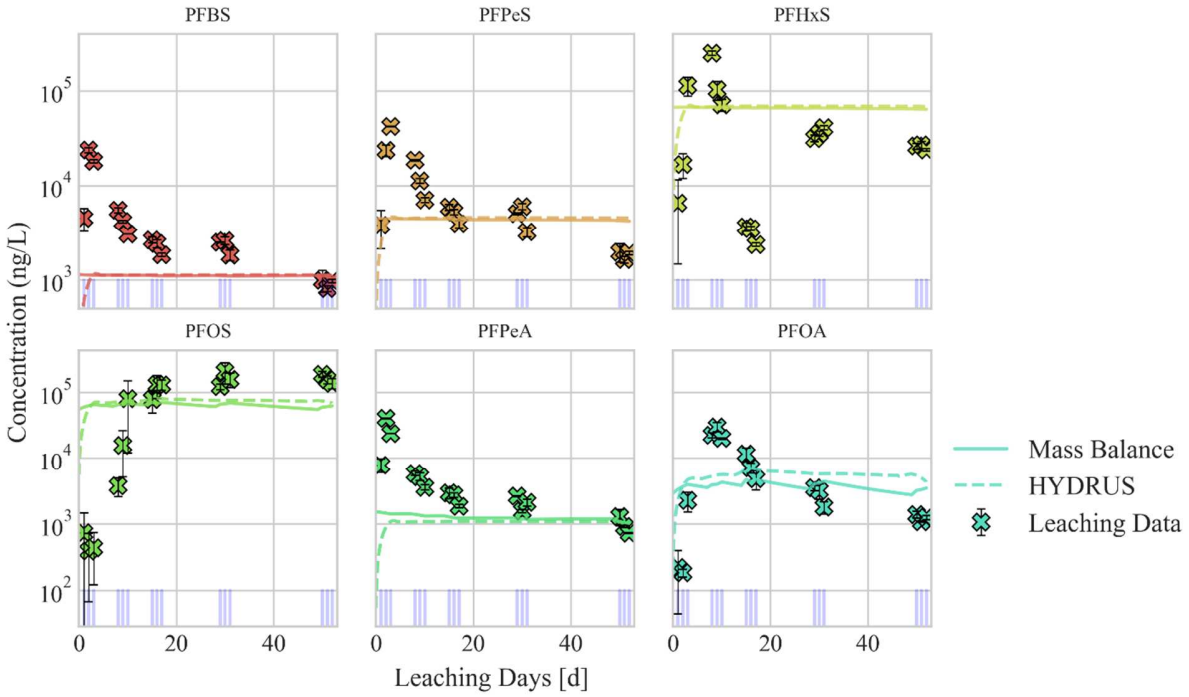

408

409 **Figure 2:** Equilibrium simulations of PFAS leaching data from the calibrated HYDRUS (dashed line) model and the Freundlich
410 mass balance model (solid line) from the measured outflow and estimated water content data. Leaching data points are averages
411 of concentrations measured from duplicate experiments and error bars represent the standard deviation of concentration between
412 two experiments. Blue lines indicate rainfall events.

413 Both the total mass flux (Figure S.13) and the late time concentrations (see late time data
414 of 20-60 days) are well predicted within a factor of 3 by both the mass balance model and the
415 equilibrium HYDRUS model for all components except PFBS and PFPeA. These findings
416 suggest that in the long term (greater than 50 days in this case), equilibrium averaging models
417 may be able to capture total mass leaching of PFAS from the vadose zone assuming there is
418 sufficient calibration and transport data for the field site. PFBS total mass flux is underpredicted
419 by the mass balance model is potentially because the non-labile mass fraction is overestimated.
420 PFPeA was likely impacted by precursor transformation (as noted by the cumulative mass
421 increasing to over 100% in Figure S.11) and thus also suffered from incomplete mass balance
422 information. This finding is consistent with the presence of known PFPeA precursor (6:2 FTS) at
423 concentration 10x higher than PFPeA (Yang et al., 2022). Importantly, simplistic mass balance

calculations were in excellent agreement with HYDRUS predictions (Figures 2 and S.13), suggesting at field sites which can be simulated using equilibrium partitioning processes may not require comprehensive leaching models to effectively assess PFAS loading to the groundwater.

Neither the water flux calibrated HYDRUS model nor the mass balance model adequately captures trends in concentration associated with PFAS. All equilibrium models predict that PFAS porewater concentrations should remain relatively constant over time with small decreases in porewater concentration associated with excessive drying periods. This is contrary to the theory of evapoconcentration, which would suggest that decreased porewater saturation should result in higher concentrations of PFAS in bulk porewater. This apparent contradiction in model results can be explained by the formation of air-water interfaces in the column with decreasing water content within the pore space, which strongly retain PFAS. Evapoconcentration effects would not appear in the eluate results either, as samples only eluate samples collected during major rainfall events, thus negating the evapoconcentration effect, could be analyzed. It is unclear whether PFAS retained at the air-water interface will be readily extracted by field lysimeter techniques, resulting in elevated porewater concentrations measured at vadose zone sites. However, this does suggest that air-water interfacial formation and collapse will be important determinants of PFAS porewater concentration in the vadose zone.

Inversion Based Identification of Non-Equilibrium Transport Mechanisms

Model inversion of the three (Freundlich AWIA, no AWIA, linear AWIA) two-site kinetic models were implemented for each of the six PFAS components (18 total models). The goodness of fit was assessed using AIC weights with the R^2 provided as a supplementary goodness of fit measure. The summary of goodness of fit data for each model are presented in Table 3 and full model inversion results are presented in Tables S.6-8.

Table 3 Summary of the goodness of fit terms. The bolded items have a high wAIC confidence (wAIC > 0.9) for the model appropriateness. Because R^2 values are not optimized for non-linear problems, we prefer to rely on the AIC/wAIC metric for evaluating best fit of various models.

		Fit Criteria		
Model	Component	R2	AIC	wAIC
Model 1 (Freundlich AWIA)	PFPeA	0.170	-93.4	0.54
	PFOA	0.003	-93.8	0.00
	PFBS	**0.506**	**-104.2**	**0.91**
	PFPeS	0.289	-88.9	0.00
	PFHxS	0.484	48.3	0.00
	PFOS	**0.400**	**-40**	**0.92**
Model 2 (No AWIA)	PFPeA	0.011	-91.7	0.23
	PFOA	0.154	-98.3	0.00
	PFBS	0.268	-97.8	0.04
	PFPeS	0.676	-114	0.03
	PFHxS	**0.519**	**-52.5**	**1.00**
	PFOS	0.009	-6.6	0.00
Model 3 (Linear AWIA)	PFPeA	0.021	-91.7	0.23
	PFOA	**0.607**	**-112**	**1.00**
	PFBS	0.289	-98.3	0.05
	PFPeS	**0.791**	**-121**	**0.97**
	PFHxS	0.558	-36.1	0.00
	PFOS	0.321	-35.1	0.08

The three alternative models had mixed performance across several PFAS, with Model 2 (no AWIA) performing comparatively well for all PFAS except PFOS and PFOA. This finding demonstrates that rate-limited desorption from solids is likely a much more important determinant of leaching behavior for short chain PFAS than air-water interfacial partitioning. In particular, Model 2 was best able to capture the anomalous leaching behavior of PFHxS, which experienced a sharp drop in concentration over the third rainfall event followed by steady increase in concentration with the 4th and 5th event. Model performance for the components with the highest air-water interfacial partitioning (PFOS and PFOA) were split, with Model 1 (Freundlich) significantly outperforming Model 3 (Langmuir) for PFOS, and vice versa for PFOA. Model 3 generally had the highest average R^2 values, but AIC results were generally

mixed between models. These discrepancies may be attributable to rate-limited desorption from air-water interfaces (Stults et al., 2023), competitive adsorption to air-water interfaces (Abraham et al., 2022; Guo et al., 2023), anomalous adsorption to air-water interfaces (Zhang and Guo, 2024), or other non-Fickian processes (Hasan et al., 2019; Stults et al., 2021; Zeng and Guo, 2023) which could not be investigated with HYDRUS or using the data in this dataset. To better understand how solid desorption and air-water interfacial collapse drive PFAS leaching behavior, optimized Models 1 and 3 are plotted against the measured effluent data for the PFAAs in Figure 3.

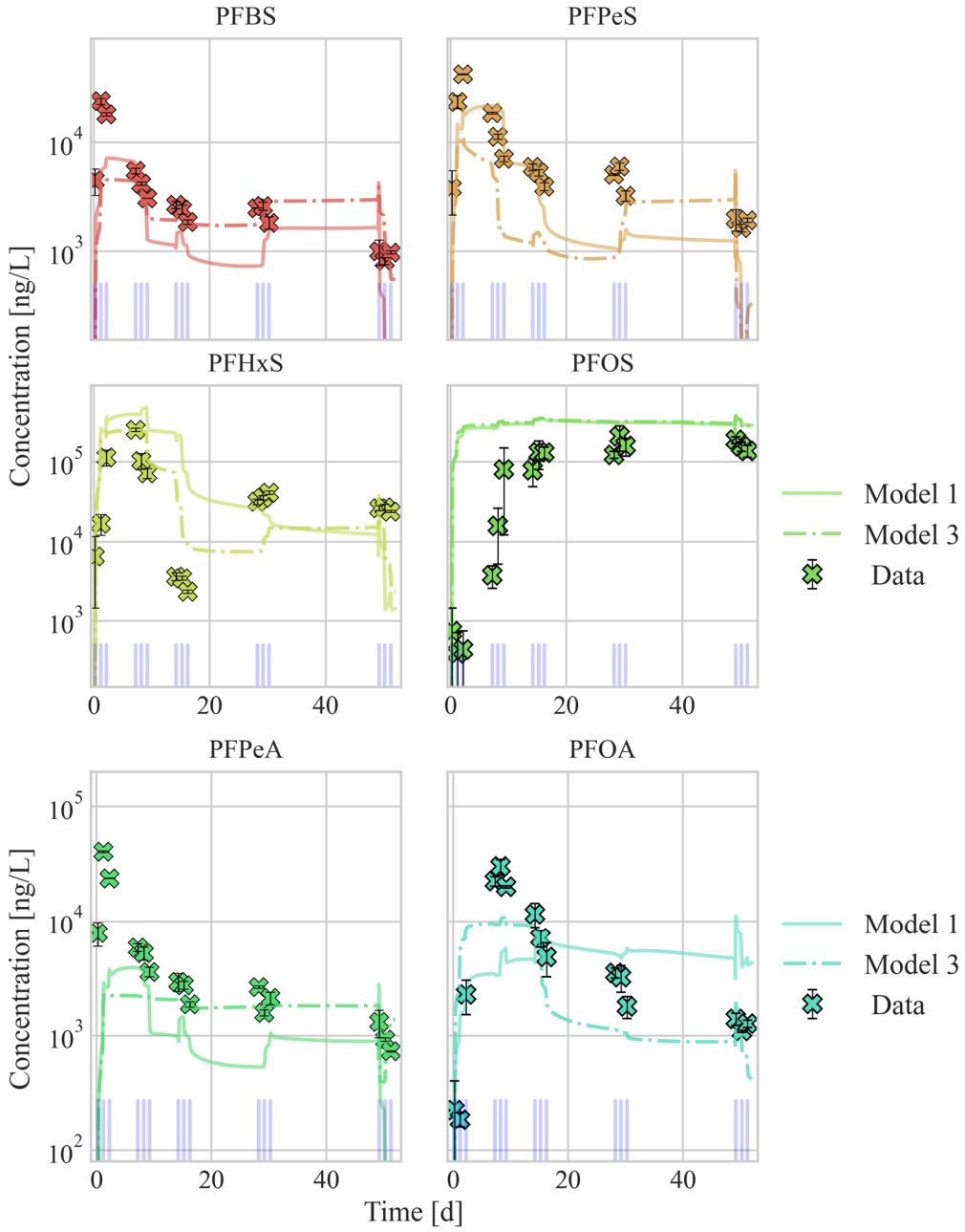

Figure 3a-b: (a-top) Model inversion results for PFSAs for models 1 & 3. **(b-bot)** Model inversion results for PFCAs for models 1 & 3. Blue lines at the base of the figure represent rain events.

Model 1 and Model 3 showed distinctly different leaching behavior (Figure 3), while Model 2 & Model 3 were very similar for every component except PFOS & PFOA (Figure S.14). Model 1 and Model 3 show spikes in concentration during the wetting pulses due to the collapse

475 of air-water interfaces in the porous media. Contrary to what was suggested by the wAIC values,
476 only Model 1 and Model 3 have relatively similar predictions for PFOS .

477 Because of the high degree of uncertainty related to mixture effects, and uncertainty
478 regarding rate-limited or anomalous air-water interfacial partitioning, both the mass transfer rates
479 and f values should be considered order of magnitude approximations of what may be
480 empirically measured. PFPeA concentrations were significantly under predicted by the model
481 likely due to precursor transformation (Figures S.11-S.12), and thus none of the proposed model
482 performed very well in simulating PFPeA transport. The long chain PFOS and PFOA predictions
483 show very distinct behaviors despite being the most hydrophobic and air-water interfacially
484 active of the two components. This is potentially due to mixture effects at the air-water interface,
485 wherein PFOS adsorption to the interface may reduce the number of sites available for PFOA
486 and other short chain components (Guo et al., 2023).

487 Short chain PFAAs and PFOA were rapidly released during the first and second rain
488 events respectively. These results are highly dynamic and suggest that site competition effects
489 may be present in this system for the solid phase (Piñeiro et al., 2001). This is supported by the
490 inverse parameter estimation results, which predict the best estimations of PFAA transport
491 require less than 1% of all sites as equilibrium adsorption sites (Tables S.6-8). While only six
492 PFAAs had sufficient data quality to justify an attempt at modelling these complex and highly
493 dynamic systems, this AFFF impacted soil is known to have dozens of other PFAS (PFAAs as
494 well as PFAA precursors) present in the mixture (Maizel et al., 2021; Schaefer et al., 2021).
495 Adsorption site competition effectively lowers the apparent solid and air-water interfacial
496 partitioning coefficients for less strongly adsorbed components when present in mixtures. This
497 effect of multi-component mixtures on adsorption to the air-water interface has been quantified

with modeling (Guo et al., 2023) and experimentally (Abraham et al., 2022; Huang et al., 2022; Lyu et al., 2022). Site adsorption competition to the solid interface has not been measured to the best of our knowledge, but is predicted to occur at high total PFAS concentrations based on the theory of the extend (multi-component) Langmuir isotherm (Piñeiro et al., 2001). Other possible explanations for the highly dynamic leaching include anomalous adsorption to thin films in the media during wetting and drying cycles (Zhang and Guo, 2024), and that the column may not have been uniformly loaded despite the best efforts to achieve uniform soil distributions in the column.

Sensitivity Analysis of Initial Conditions, Equilibrium Mass Fraction, and Rate Limitation

Because the highly dynamic nature of these columns and the flexible nature of parameter inversion, a sensitivity analysis was conducted to determine the impact of initial conditions specification and the two parameters estimated via inversion [(f) and (α_k)]. PFPeS and PFOS were selected for sensitivity analysis based on their representativeness of components which were weakly adsorbed to air-water interfaces and strongly adsorbed to air-water interfaces respectively. PFPeS sensitivity analysis was conducted at with two labile mass fraction values (f = 0, 0.01), four rate-limited desorption values (α_k = 1e-2, 1e-4, 1e-6, 1e-8 min^{-1}), with and without air-water interfacial adsorption, and considering mass that was initially at equilibrium vs. mass that was not initially at equilibrium and defined explicitly based on the labile mass fraction values. The K_d and K_{ia} defined in Table 2 were used for the PFPeS simulations. A Freundlich isotherm was used for all sensitivity analysis simulations to provide significantly different comparison to sensitivity without air-water interfacial adsorption. Note that all inversions-based models assumed that the non-equilibrium and equilibrium phases were initially at equilibrium.

The input values for the sensitivity analysis are presented in Table 3 and results are presented in Figure 4a-h.

Table 3: Information on the input parameters for the PFPeS sensitivity analysis. For simulations where PFAS mass was initially at equilibrium with all domains the total concentration of PFAS mass in the system could be specified for HYDRUS. For simulations where initial equilibrium was not assumed total equilibrium concentration and the kinetically adsorbed concentration needed to be assumed.

Case	f (-)	αk (1/min)	Total Conc. (ng/g)	Total Eq. Conc. (ng/mL)	Kinetic Conc. (ng/g)	Kaw [cm /(ng/mL)$^{-.35}$]	β_a[-]	Kd [cm^3/g]
Not at Equilibrium	0	1e-2, 1e-4, 1e-6, 1e-8	n.a.	0.00	53.41	0.0084	0.65	5.7
Initially Equilibrium	0	1e-2, 1e-4, 1e-6, 1e-8	53.41	n.a.	n.a.			
Not at Equilibrium	0.01	1e-2, 1e-4, 1e-6, 1e-8	n.a.	0.53	52.88			
Initially Equilibrium	0.01	1e-2, 1e-4, 1e-6, 1e-8	53.41	n.a.	n.a.			
Not at Equilibrium	0	1e-2, 1e-4, 1e-6, 1e-8	n.a.	0.00	53.41	0	1	5.7
Initally Equilibrium	0	1e-2, 1e-4, 1e-6, 1e-8	53.41	n.a.	n.a.			
Not at Equilibrium	0.01	1e-2, 1e-4, 1e-6, 1e-8	n.a.	0.53	52.88			
Initally Equilibrium	0.01	1e-2, 1e-4, 1e-6, 1e-8	53.41	n.a.	n.a.			

f is the fraction of equilibrium adsorption sites and labile mass, K_{aw} is the Freundlich air-water interfacial partitioning coefficent, β_a is the Freundlich non-linearity term for the air-water interfacial partitioning coefficient

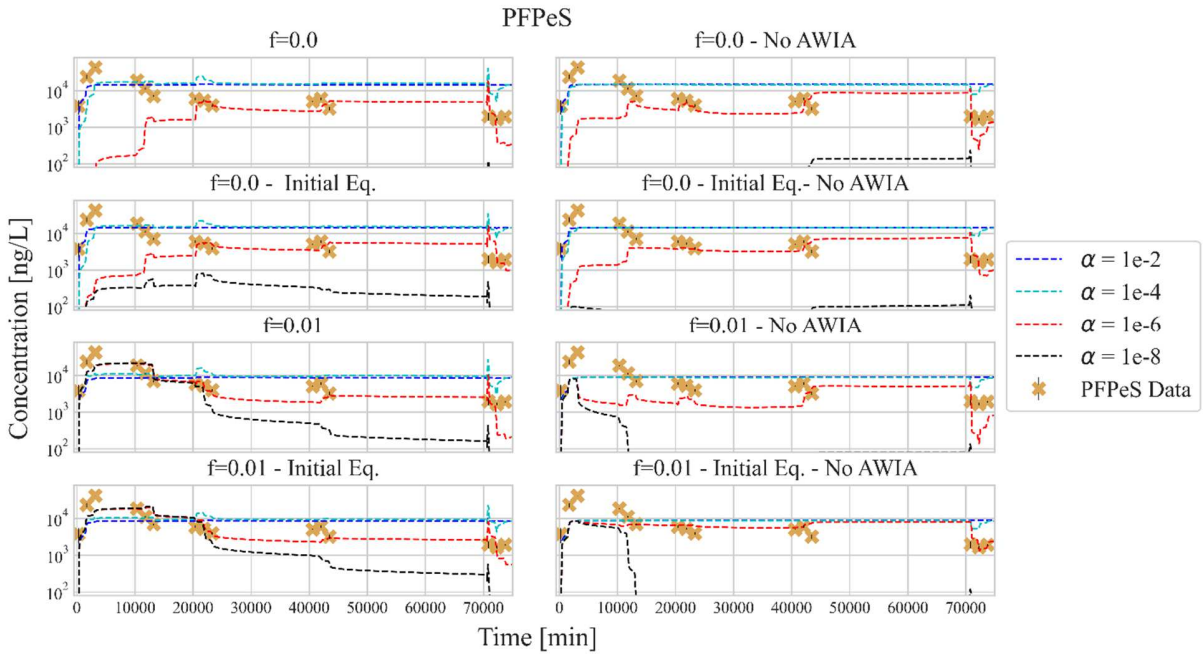

528

529 **Figure 4a-h**: From left to right and top to bottom: (a) PFPeS simulations using the Freundlich isotherm for air-water interfacial
530 partitioning with 0% equilibrium sites; (b) PFPeS simulations using with no air-water interfacial partitioning with 0% equilibrium
531 sites; (c) PFPeS simulations using the Freundlich isotherm for air-water interfacial partitioning with 0% equilibrium sites and
532 mass initially at equilibrium; (d) PFPeS simulations using with no air-water interfacial partitioning with 0% equilibrium sites and
533 mass initially at equilibrium; (e) PFPeS simulations using the Freundlich isotherm for air-water interfacial partitioning with 1%
534 equilibrium sites; (f) PFPeS simulations using with no air-water interfacial partitioning with 1% equilibrium sites; (g) PFPeS
535 simulations using the Freundlich isotherm for air-water interfacial partitioning with 1% equilibrium sites and mass initially at
536 equilibrium; (h) PFPeS simulations using with no air-water interfacial partitioning with 1% equilibrium sites and mass initially at
537 equilibrium.

538 Results from the sensitivity analysis show that the assumption of initial equilibrium and
539 non-equilibrium phases can significantly alter the results for components with significant rate
540 limitations (α_k <0.0001 1/min). These results also demonstrate the despite poorer performance of
541 the Freundlich isotherm for PFPeS in the inversion data, the Freundlich isotherm can still
542 produce reasonable simulations of PFPeS leaching under highly dynamic conditions. We also
543 demonstrate that treating even a small fraction (1%) of sites as equilibrium vs. entirely non-
544 equilibrium can drastically alter the results of both simulations. Based on the sensitivity analysis
545 and results from numerical inversion (Tables S.6-8), it appears that much of the dynamic
546 leaching observed in the early stages of the experiment is driven by a small portion of
547 equilibrium mass rapidly being released form the column in the first wetting event, followed by a

548 slowly desorbed rate limited mass fraction controlling the later time behavior. The most
549 appropriate rate limited constant was the red line representing a rate limitation of 1e-6 min^{-1},
550 which is in good agreement with a rate limited desorption coefficient of 5 e-6 min^{-1} measured in
551 previous studies on this soil (Schaefer et al., 2021). The difference between the simulations
552 which considered air-water interfacial partitioning and those that did not were small but
553 noticeable in this sensitivity analysis. This in good agreement with mass distribution calculations
554 for the initial conditions, which predict that approximately 3% of the total mass is initially
555 adsorbed to air-water interfaces, and 1% of the mass is in the aqueous phase. Contrary to what
556 was predicted by numerical inversion, the simulations which consider the Freundlich isotherm
557 for the air-water interface and initial equilibrium appear to give reasonable estimates of the
558 trends of PFPeS elution profiles.

559 Because it was observed that setting the equilibrium and non-equilibrium solute mass to
560 initially be at equilibrium produced significantly different results from explicitly defining the
561 mass in each compartment, it was decided to simulate PFOS sensitivity results initially not at
562 equilibrium. It was theorized that the slow increase in PFOS mass observed during the first two
563 rain events was likely the result of significant rate limitation, invalidating the assumption of
564 initial equilibrium between the non-equilibrium and equilibrium adsorption sites. The full form
565 of the Freundlich isotherm was used for the PFOS simulations as it was observed that the
566 Freundlich isotherm had higher performance than other models for PFOS. Results of the PFOS
567 sensitivity analysis are presented in Table 4 and figures 5a-h.

568

Table 4: Information on the input parameters for the PFPeS sensitivity analysis.

Case	f (-)	αk (1/min)	Total Eq. Conc. (ng/g)	Kinetic Conc. (ng/g)	Kaw [cm /(ng/mL)$^{-.35}$]	β_a [-]	Kd [cm^3/g]
Not at Equilibrium	0	1e-2, 1e-4, 1e-6, 1e-8	0.00	2590	0.3	0.65	6.9
Not at Equilibrium	0.01	1e-2, 1e-4, 1e-6, 1e-8	26	2564			
Not at Equilibrium	0.1	1e-2, 1e-4, 1e-6, 1e-8	259	2331			
Not at Equilibrium	0.9	1e-2, 1e-4, 1e-6, 1e-8	2331	259			
Not at Equilibrium	0	1e-2, 1e-4, 1e-6, 1e-8	0.00	2590	0	1	6.9
Not at Equilibrium	0.01	1e-2, 1e-4, 1e-6, 1e-8	26	2564			
Not at Equilibrium	0.1	1e-2, 1e-4, 1e-6, 1e-8	259	2331			
Not at Equilibrium	0.9	1e-2, 1e-4, 1e-6, 1e-8	2331	259			

f is the fraction of equilibrium adsorption sites and labile mass, K_{aw} is the Freundlich air-water interfacial partitioning coefficent, β_a is the Freundlich non-linearity term for the air-water interfacial partitioning coefficient.

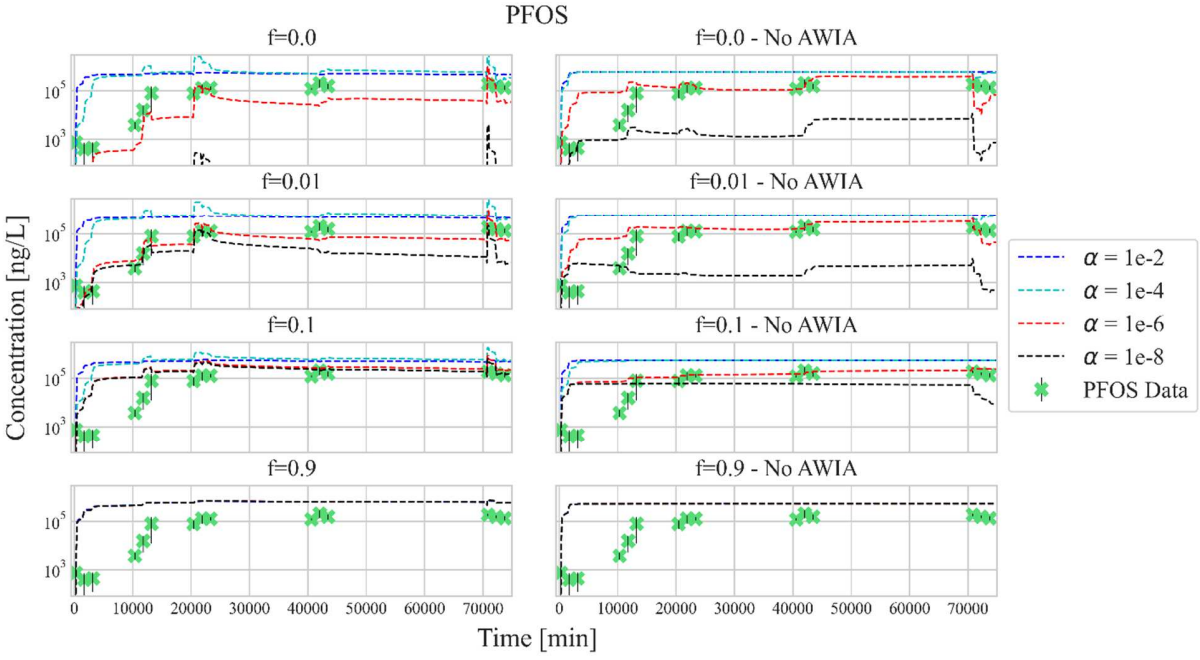

Figure 5a-h: From left to right and top to bottom: (a) PFOS simulations using the Freundlich isotherm for air-water interfacial partitioning with 0% equilibrium sites; (b) PFOS simulations using with no air-water interfacial partitioning with 0% equilibrium sites; (c) PF)S simulations using the Freundlich isotherm for air-water interfacial partitioning with 1% equilibrium sites; (d) PFOS simulations using with no air-water interfacial partitioning with 1% equilibrium sites; (e) PFOS simulations using the Freundlich isotherm for air-water interfacial partitioning with 10% equilibrium sites; (f) PFOS simulations using with no air-water interfacial partitioning with 10% equilibrium sites; (g) PFOS simulations using the Freundlich isotherm for air-water

interfacial partitioning with 90% equilibrium sites; (h) PFOS simulations using with no air-water interfacial partitioning with 90% equilibrium sites.

Figure 5 demonstrates that the full Freundlich isotherm for air-water interfacial adsorption coupled with strictly defined mass distributions between the equilibrium and non-equilibrium phases can accurately quantify PFAS leaching. At low equilibrium mass fractions, each model is very sensitive to the value of the rate-limited desorption term. As the equilibrium mass fraction increases, the solutions all naturally converge on one another as the equilibrium partitioning begins to dominate any rate limited desorption effects for strongly retained PFAS. The solutions demonstrate that simulation with an equilibrium mass fraction of 1% with a moderate to high rate-limitation of 1e-6 to 1e-8 min^{-1} produce simulation results which are most well correlated with observed values. This is in excellent agreement with prior results, which the rate limited coefficient of desorption is around 5e-7 min^{-1} (Schaefer et al, 2021, 2022c). For both PFOS and PFPeS sensitivity analysis the fraction of equilibrium mass that is most likely was around 1% or less (Tables S.6-8). This is much less than the fraction of equilibrium mass measured for saturated systems in (Schaefer et al., 2021), suggesting there may kinetically limited air water interfaces (Stults et al., 2023) or that non-Fickian, rate-limited transport is increasingly important at lower saturations (Hasan et al., 2019; Stults et al., 2021; Zeng and Guo, 2023). The degree of correlation between the simulation results of different rate-limitation coefficients increases as the fraction of equilibrium, showing how rate-limitation impacts are not observable in simulation with high degrees of equilibrium adsorption sites. In the numerical inversion results the coefficient of co-correlation between f and α_k was very low (0.05-0.2), suggesting the predicted low equilibrium adsorption sites fraction is not an artifact of simulation but a real phenomenon. Because of the extreme sensitivity to the specified initial conditions, it appears the simulation of rate limited desorption from soils is an ill-posed inverse problem.

Conclusions

Equilibrium models of leaching which consider labile and non-labile mass fractions were able to estimate the total mass released from column systems using simplified mass balance models and equilibrium partitioning data determined in laboratory settings (Schaefer et al., 2021; Stults et al., 2023). This is consistent with modelling studies which suggest water flux and equilibrium partitioning can capture the long term (> 50 days) behavior of PFAS in the vadose zone (Wallis et al., 2022; Zeng and Guo, 2023). However, equilibrium models performed poorly with respect to predicting column effluent porewater concentrations, demonstrating that equilibrium partitioning models do not fully capture the desorption mechanisms of PFAS from historically impacted soils. A conceptual model was developed which incorporated the concepts of labile (equilibrium) and non-labile (non-equilibrium) PFAS mass as well as rate-limited desorption from soils (Schaefer et al., 2021). The behavior of short chain PFAS leaching appears to be primarily controlled by the effect of rate-limited desorption from soil and precursor transformation, with air-water interfacial partitioning playing a less pronounced role in the observed desorption behavior. The amount of labile vs. non-labile mass also appears to plays an important role in the behavior of PFAS leaching from soils. The impact of AWIA on transport was very important for describing longer chain PFAA leaching from soils (PFOA, PFOS). While the results of this modelling are not conclusive evidence supporting the Freundlich or Langmuir isotherm, all the modelling results emphasize that air-water interfacial collapse is an important mechanism controlling the leaching of PFAS. The Freundlich model which considered significant rate limitation was able to able to accurately capture PFOS behavior, while the Langmuir model was able to more accurately capture PFOA behavior via inversion. It is not clear why there is a discrepancy in model estimation between these two well-studied PFAS, but

it is likely that mixture effects play a significant role in controlling the air-water interfacial partitioning behavior for this system (Guo et al., 2023). Equilibrium models were able to obtain reasonable estimations of long-term mass flux and concentrations for some PFAS when the non-labile mass fraction was considered. This suggests the need for full numerical simulation of air-water interfacial collapse and rate limited desorption may be project or site specific. We also note that dual-equilibrium desorption models are an alternative to modelling rate-limited desorption from soils without the need for explicit rate limitation constants (Chen et al., 2002; Kan et al., 1997).

A great deal of uncertainty still exists with respect to the mechanisms of PFAS desorption from historically impacted soils. None of the models presented herein allowed for rate-limited mass transfer from air-water interfacial domains. Recent pore scale modelling evidence has suggested that in drier soils this rate-limited mass transfer from air-water interfaces could affect PFAS desorption (Ben-Noah et al., 2023; Chen and Guo, 2023; Hasan et al., 2019). The model presented here-in also could not be fully validated due limitations with HYDRUS. The two-site kinetic limitation model is advantageous because of its simplicity relative to other non-Fickian transport models (TOSD, MRMT), but does not fully elucidate why mass transfer is so dramatically different between PFAS. Initial evidence suggests aqueous diffusivity plays a role in determining the mass transfer coefficient (Schaefer et al., 2021), supporting the application of an MRMT or MIM based model. Other significant uncertainties in this work relate to the impact of hysteresis on flow and air-water interfacial areas (Schaefer et al., 2000; Zhuang et al., 2017) and the effect of anomalous adsorption to thin film interfaces (Zhang and Guo, 2024). Because of these modeling uncertainties, it may be advantageous for site managers to implement equilibrium models partitioning at field sites where inherent uncertainty compounds the effect of

649 modelling uncertainty. Equilibrium models likely cannot predict large releases from discrete
650 storm events but appear to give a reasonable assessment of long-term leaching potential under
651 controlled conditions.

652 **Acknowledgments**

653 Funding was provided by SERDP project ER20-1126. Opinions of the authors are not our own
654 and not those of SERDP.

655

656

657

658

659

660

661

662

663

664

665

666

667

References

Abraham, J.E.F., Mumford, K.G., Patch, D.J., Weber, K.P., 2022. Retention of PFOS and PFOA Mixtures by Trapped Gas Bubbles in Porous Media. Environ. Sci. Technol. 56, 15489–15498. https://doi.org/10.1021/acs.est.2c00882

Anderson, R.H., Long, G.C., Porter, R.C., Anderson, J.K., 2016. Occurrence of select perfluoroalkyl substances at U.S. Air Force aqueous film-forming foam release sites other than fire-training areas: Field-validation of critical fate and transport properties. Chemosphere 150, 678–685. https://doi.org/10.1016/j.chemosphere.2016.01.014

Arshadi, M., Costanza, J., Abriola, L.M., Pennell, K.D., 2020. Comment on "Uptake of Poly- and Perfluoroalkyl Substances at the Air–Water Interface." Environ. Sci. Technol. 54, 7019–7020. https://doi.org/10.1021/acs.est.0c01838

Ben-Noah, I., Hidalgo, J.J., Jimenez-Martinez, J., Dentz, M., 2023. Solute Trapping and the Mechanisms of Non-Fickian Transport in Partially Saturated Porous Media. Water Resources Research 59. https://doi.org/10.1029/2022WR033613

Brusseau, M.L., 2023a. Influence of chain length on field-measured distributions of PFAS in soil and soil porewater. Journal of Hazardous Materials Letters 4, 100080. https://doi.org/10.1016/j.hazl.2023.100080

Brusseau, M.L., 2023b. Determining air-water interfacial areas for the retention and transport of PFAS and other interfacially active solutes in unsaturated porous media. Science of The Total Environment 884, 163730. https://doi.org/10.1016/j.scitotenv.2023.163730

Brusseau, M.L., 2018. Assessing the potential contributions of additional retention processes to PFAS retardation in the subsurface. Science of The Total Environment 613–614, 176–185. https://doi.org/10.1016/j.scitotenv.2017.09.065

Brusseau, M.L., Anderson, R.H., Guo, B., 2020. PFAS concentrations in soils: Background levels versus contaminated sites. Science of The Total Environment 740, 140017. https://doi.org/10.1016/j.scitotenv.2020.140017

Brusseau, M.L., Guo, B., 2022. PFAS concentrations in soil versus soil porewater: Mass distributions and the impact of adsorption at air-water interfaces. Chemosphere 302, 134938. https://doi.org/10.1016/j.chemosphere.2022.134938

Brusseau, M.L., Guo, B., 2021. Air-water interfacial areas relevant for transport of per and poly-fluoroalkyl substances. Water Research 207, 117785. https://doi.org/10.1016/j.watres.2021.117785

Brusseau, M.L., Guo, B., Huang, D., Yan, N., Lyu, Y., 2021. Ideal versus Nonideal Transport of PFAS in Unsaturated Porous Media. Water Research 202, 117405. https://doi.org/10.1016/j.watres.2021.117405

Brusseau, M.L., Khan, N., Wang, Y., Yan, N., Van Glubt, S., Carroll, K.C., 2019. Nonideal Transport and Extended Elution Tailing of PFOS in Soil. Environ. Sci. Technol. 53, 10654–10664. https://doi.org/10.1021/acs.est.9b02343

Brusseau, M.L., Rao, P.S.C., 1989. Sorption nonideality during organic contaminant transport in porous media. Critical Reviews in Environmental Control 19, 33–99. https://doi.org/10.1080/10643388909388358

Chen, S., Guo, B., 2023. Pore-Scale Modeling of PFAS Transport in Water-Unsaturated Porous Media: Air–Water Interfacial Adsorption and Mass-Transfer Processes in Thin Water Films. Water Resources Research 59, e2023WR034664. https://doi.org/10.1029/2023WR034664

712 Chen, W., Kan, A.T., Newell, C.J., Moore, E., Tomson, M.B., 2002. More Realistic Soil Cleanup Standards
713 with Dual-Equilibrium Desorption. Groundwater 40, 153–164. https://doi.org/10.1111/j.1745-
714 6584.2002.tb02500.x
715 Faust, J.A., 2023. PFAS on atmospheric aerosol particles: a review. Environ. Sci.: Processes Impacts 25,
716 133–150. https://doi.org/10.1039/D2EM00002D
717 Fenton, S.E., Ducatman, A., Boobis, A., DeWitt, J.C., Lau, C., Ng, C., Smith, J.S., Roberts, S.M., 2021. Per-
718 and Polyfluoroalkyl Substance Toxicity and Human Health Review: Current State of Knowledge
719 and Strategies for Informing Future Research. Environ Toxicol Chem 40, 606–630.
720 https://doi.org/10.1002/etc.4890
721 Glüge, J., Scheringer, M., Cousins, I.T., DeWitt, J.C., Goldenman, G., Herzke, D., Lohmann, R., Ng, C.A.,
722 Trier, X., Wang, Z., 2020. An overview of the uses of per- and polyfluoroalkyl substances (PFAS).
723 Environ. Sci.: Processes Impacts 22, 2345–2373. https://doi.org/10.1039/D0EM00291G
724 Guelfo, J.L., Adamson, D.T., 2018. Evaluation of a national data set for insights into sources,
725 composition, and concentrations of per- and polyfluoroalkyl substances (PFASs) in U.S. drinking
726 water. Environmental Pollution 236, 505–513. https://doi.org/10.1016/j.envpol.2018.01.066
727 Guelfo, J.L., Korzeniowski, S., Mills, M.A., Anderson, J., Anderson, R.H., Arblaster, J.A., Conder, J.M.,
728 Cousins, I.T., Dasu, K., Henry, B.J., Lee, L.S., Liu, J., McKenzie, E.R., Willey, J., 2021. Environmental
729 Sources, Chemistry, Fate, and Transport of Per- and Polyfluoroalkyl Substances: State of the
730 Science, Key Knowledge Gaps, and Recommendations Presented at the August 2019 SETAC
731 Focus Topic Meeting. Enviro Toxic and Chemistry 40, 3234–3260.
732 https://doi.org/10.1002/etc.5182
733 Guelfo, J.L., Wunsch, A., McCray, J., Stults, J.F., Higgins, C.P., 2020. Subsurface transport potential of
734 perfluoroalkyl acids (PFAAs): Column experiments and modeling. Journal of Contaminant
735 Hydrology 233, 103661. https://doi.org/10.1016/j.jconhyd.2020.103661
736 Guo, B., Saleem, H., Brusseau, M.L., 2023. Predicting Interfacial Tension and Adsorption at Fluid–Fluid
737 Interfaces for Mixtures of PFAS and/or Hydrocarbon Surfactants. Environ. Sci. Technol. 57,
738 8044–8052. https://doi.org/10.1021/acs.est.2c08601
739 Hasan, S., Joekar-Niasar, V., Karadimitriou, N.K., Sahimi, M., 2019. Saturation Dependence of Non-
740 Fickian Transport in Porous Media. Water Resources Research 55, 1153–1166.
741 https://doi.org/10.1029/2018WR023554
742 Hasan, S., Niasar, V., Karadimitriou, N.K., Godinho, J.R.A., Vo, N.T., An, S., Rabbani, A., Steeb, H., 2020.
743 Direct characterization of solute transport in unsaturated porous media using fast X-ray
744 synchrotron microtomography. Proceedings of the National Academy of Sciences of the United
745 States of America 117, 23443–23449. https://doi.org/10.1073/pnas.2011716117
746 Høisæter, Å., Pfaff, A., Breedveld, G.D., 2019. Leaching and transport of PFAS from aqueous film-forming
747 foam (AFFF) in the unsaturated soil at a firefighting training facility under cold climatic
748 conditions. Journal of Contaminant Hydrology 222, 112–122.
749 https://doi.org/10.1016/j.jconhyd.2019.02.010
750 Huang, D., Saleem, H., Guo, B., Brusseau, M.L., 2022. The impact of multiple-component PFAS solutions
751 on fluid-fluid interfacial adsorption and transport of PFOS in unsaturated porous media. Science
752 of The Total Environment 806, 150595. https://doi.org/10.1016/j.scitotenv.2021.150595
753 Huang, Y.-R., Liu, S.-S., Zi, J.-X., Cheng, S.-M., Li, J., Ying, G.-G., Chen, C.-E., 2023. *In Situ* Insight into the
754 Availability and Desorption Kinetics of Per- and Polyfluoroalkyl Substances in Soils with Diffusive
755 Gradients in Thin Films. Environ. Sci. Technol. 57, 7809–7817.
756 https://doi.org/10.1021/acs.est.2c09348
757 Islam, M., Thompson, K., Dickenson, E., Quiñones, O., Steinle-Darling, E., Westerhoff, P., 2023. Sucralose
758 and Predicted De Facto Wastewater Reuse Levels Correlate with PFAS Levels in Surface Waters.
759 Environ. Sci. Technol. Lett. 10, 431–438. https://doi.org/10.1021/acs.estlett.3c00185

760 Jacques, D., Smith, C., Šimůnek, J., Smiles, D., 2012. Inverse optimization of hydraulic, solute transport,
761 and cation exchange parameters using HP1 and UCODE to simulate cation exchange. Journal of
762 Contaminant Hydrology 142–143, 109–125. https://doi.org/10.1016/j.jconhyd.2012.03.008
763 Johansson, J.H., Salter, M.E., Acosta Navarro, J.C., Leck, C., Nilsson, E.D., Cousins, I.T., 2019. Global
764 transport of perfluoroalkyl acids *via* sea spray aerosol. Environ. Sci.: Processes Impacts 21, 635–
765 649. https://doi.org/10.1039/C8EM00525G
766 Kan, A.T., Fu, G., Hunter, M.A., Tomson, M.B., 1997. Irreversible Adsorption of Naphthalene and
767 Tetrachlorobiphenyl to Lula and Surrogate Sediments. Environ. Sci. Technol. 31, 2176–2185.
768 https://doi.org/10.1021/es9601954
769 Knight, E.R., Janik, L.J., Navarro, D.A., Kookana, R.S., McLaughlin, M.J., 2019. Predicting partitioning of
770 radiolabelled 14C-PFOA in a range of soils using diffuse reflectance infrared spectroscopy.
771 Science of The Total Environment 686, 505–513.
772 https://doi.org/10.1016/j.scitotenv.2019.05.339
773 Kookana, R.S., Navarro, D.A., Kabiri, S., McLaughlin, M.J., 2022. Key properties governing sorption–
774 desorption behaviour of poly- and perfluoroalkyl substances in saturated and unsaturated soils:
775 a review. Soil Res. 61, 107–125. https://doi.org/10.1071/SR22183
776 Lang, J.R., Allred, B.M., Field, J.A., Levis, J.W., Barlaz, M.A., 2017. National Estimate of Per- and
777 Polyfluoroalkyl Substance (PFAS) Release to U.S. Municipal Landfill Leachate. Environ. Sci.
778 Technol. 51, 2197–2205. https://doi.org/10.1021/acs.est.6b05005
779 Le, S.-T., Gao, Y., Kibbey, T.C.G., Glamore, W.C., O'Carroll, D.M., 2021. A new framework for modeling
780 the effect of salt on interfacial adsorption of PFAS in environmental systems. Science of The
781 Total Environment 796, 148893. https://doi.org/10.1016/j.scitotenv.2021.148893
782 Lyu, X., Li, Z., Wang, D., Zhang, Q., Gao, B., Sun, Y., Wu, J., 2022. Transport of perfluorooctanoic acid in
783 unsaturated porous media mediated by SDBS. Journal of Hydrology 607, 127479.
784 https://doi.org/10.1016/j.jhydrol.2022.127479
785 Lyu, Y., Brusseau, M.L., Chen, W., Yan, N., Fu, X., Lin, X., 2018. Adsorption of PFOA at the Air–Water
786 Interface during Transport in Unsaturated Porous Media. Environ. Sci. Technol. 52, 7745–7753.
787 https://doi.org/10.1021/acs.est.8b02348
788 Maizel, A.C., Shea, S., Nickerson, A., Schaefer, C., Higgins, C.P., 2021. Release of Per- and Polyfluoroalkyl
789 Substances from Aqueous Film-Forming Foam Impacted Soils. Environ. Sci. Technol. 55, 14617–
790 14627. https://doi.org/10.1021/acs.est.1c02871
791 Moody, C.A., Field, J.A., 1999. Determination of Perfluorocarboxylates in Groundwater Impacted by Fire-
792 Fighting Activity. Environ. Sci. Technol. 33, 2800–2806. https://doi.org/10.1021/es981355+
793 Newell, C.J., Stockwell, E.B., Alanis, J., Adamson, D.T., Walker, K.L., Anderson, R.H., 2023. Determining
794 groundwater recharge for quantifying PFAS mass discharge from unsaturated source zones.
795 Vadose Zone Journal 22, e20262. https://doi.org/10.1002/vzj2.20262
796 Nguyen, T.M.H., Bräunig, J., Thompson, K., Thompson, J., Kabiri, S., Navarro, D.A., Kookana, R.S.,
797 Grimison, C., Barnes, C.M., Higgins, C.P., McLaughlin, M.J., Mueller, J.F., 2020. Influences of
798 Chemical Properties, Soil Properties, and Solution pH on Soil–Water Partitioning Coefficients of
799 Per- and Polyfluoroalkyl Substances (PFASs). Environ. Sci. Technol. 54, 15883–15892.
800 https://doi.org/10.1021/acs.est.0c05705
801 Piñeiro, Á., Brocos, P., Amigo, A., Gracia-Fadrique, J., Guadalupe Lemus, M., 2001. Extended Langmuir
802 Isotherm for Binary Liquid Mixtures. Langmuir 17, 4261–4266.
803 https://doi.org/10.1021/la001210s
804 Richards, L.A., 1931. Capillary conduction of liquids through porous mediums. Journal of Applied Physics
805 1, 318–333. https://doi.org/10.1063/1.1745010

Ross, I., McDonough, J., Miles, J., Storch, P., Kochunarayanan, P.T., Kalve, E., Hurst, J., Dasgupta, S.S., Burdick, J., 2018. A review of emerging technologies for remediation of PFASs. Remediation 28, 101–126. https://doi.org/10.1002/rem.21553

Ruyle, B.J., Thackray, C.P., Butt, C.M., LeBlanc, D.R., Tokranov, A.K., Vecitis, C.D., Sunderland, E.M., 2023. Centurial Persistence of Forever Chemicals at Military Fire Training Sites. Environ. Sci. Technol. 57, 8096–8106. https://doi.org/10.1021/acs.est.3c00675

Schaefer, C.E., Culina, V., Nguyen, D., Field, J., 2019. Uptake of Poly- and Perfluoroalkyl Substances at the Air–Water Interface. Environ. Sci. Technol. 53, 12442–12448. https://doi.org/10.1021/acs.est.9b04008

Schaefer, C.E., DiCarlo, D.A., Blunt, M.J., 2000. Experimental measurement of air-water interfacial area during gravity drainage and secondary imbibition in porous media. Water Resour. Res. 36, 885–890. https://doi.org/10.1029/2000WR900007

Schaefer, C.E., Lavorgna, G.M., Lippincott, D.R., Nguyen, D., Christie, E., Shea, S., O'Hare, S., Lemes, M.C.S., Higgins, C.P., Field, J., 2022a. A field study to assess the role of air-water interfacial sorption on PFAS leaching in an AFFF source area. Journal of Contaminant Hydrology 248, 104001. https://doi.org/10.1016/j.jconhyd.2022.104001

Schaefer, C.E., Lavorgna, G.M., Lippincott, D.R., Nguyen, D., Schaum, A., Higgins, C.P., Field, J., 2023. Leaching of Perfluoroalkyl Acids during Unsaturated Zone Flushing at a Field Site Impacted with Aqueous Film Forming Foam. Environ. Sci. Technol. 57, 1940–1948. https://doi.org/10.1021/acs.est.2c06903

Schaefer, C.E., Lemes, M.C.S., Schwichtenberg, T., Field, J.A., 2022b. Enrichment of poly- and perfluoroalkyl substances (PFAS) in the surface microlayer and foam in synthetic and natural waters. Journal of Hazardous Materials 440, 129782. https://doi.org/10.1016/j.jhazmat.2022.129782

Schaefer, C.E., Nguyen, D., Christie, E., Shea, S., Higgins, C.P., Field, J., 2022c. Desorption Isotherms for Poly- and Perfluoroalkyl Substances in Soil Collected from an Aqueous Film-Forming Foam Source Area. J. Environ. Eng. 148, 04021074. https://doi.org/10.1061/(ASCE)EE.1943-7870.0001952

Schaefer, C.E., Nguyen, D., Christie, E., Shea, S., Higgins, C.P., Field, J.A., 2021. Desorption of Poly- and Perfluoroalkyl Substances from Soil Historically Impacted with Aqueous Film-Forming Foam. J. Environ. Eng. 147, 06020006. https://doi.org/10.1061/(ASCE)EE.1943-7870.0001846

Schaefer, C.E., Nguyen, D., Fang, Y., Gonda, N., Zhang, C., Shea, S., Higgins, C.P., 2024. PFAS Porewater concentrations in unsaturated soil: Field and laboratory comparisons inform on PFAS accumulation at air-water interfaces. Journal of Contaminant Hydrology 264, 104359. https://doi.org/10.1016/j.jconhyd.2024.104359

Schaefer, C.E., Nguyen, D., Field, J., 2020. Response to the Comment on "Uptake of Poly- and Perfluoroalkyl Substances at the Air-Water Interface." Environ. Sci. Technol. 54, 7021–7022. https://doi.org/10.1021/acs.est.0c02488

Schroth, M.H., Oostrom, M., Wietsma, T.W., Istok, J.D., 2001. In-situ oxidation of trichloroethene by permanganate: effects on porous medium hydraulic properties. Journal of Contaminant Hydrology 50, 79–98. https://doi.org/10.1016/S0169-7722(01)00098-5

Sharifan, H., Bagheri, M., Wang, D., Burken, J.G., Higgins, C.P., Liang, Y., Liu, J., Schaefer, C.E., Blotevogel, J., 2021. Fate and transport of per- and polyfluoroalkyl substances (PFASs) in the vadose zone. Science of the Total Environment 771, 145427. https://doi.org/10.1016/j.scitotenv.2021.145427

Shojaei, M., Kumar, N., Guelfo, J.L., 2022. An Integrated Approach for Determination of Total Per- and Polyfluoroalkyl Substances (PFAS). Environ. Sci. Technol. 56, 14517–14527. https://doi.org/10.1021/acs.est.2c05143

Shokri, N., Lehmann, P., Or, D., 2010. Evaporation from layered porous media. J. Geophys. Res. 115, 2009JB006743. https://doi.org/10.1029/2009JB006743

Silva, J.A.K., Šimůnek, J., McCray, J.E., 2022. Comparison of methods to estimate air-water interfacial areas for evaluating PFAS transport in the vadose zone. Journal of Contaminant Hydrology 247. https://doi.org/10.1016/j.jconhyd.2022.103984

Silva, J.A.K., Šimůnek, J., McCray, J.E., 2020. A modified hydrus model for simulating pfas transport in the vadose zone. Water (Switzerland) 12. https://doi.org/10.3390/w12102758

Sima, M.W., Jaffé, P.R., 2021. A critical review of modeling Poly- and Perfluoroalkyl Substances (PFAS) in the soil-water environment. Science of The Total Environment 757, 143793. https://doi.org/10.1016/j.scitotenv.2020.143793

Šimůnek, J., Genuchten, M.T.V., 2008. Modeling Nonequilibrium Flow and Transport Processes Using HYDRUS, Vadose Zone Journal. https://doi.org/10.2136/vzj2007.0074

Stults, J., Illangasekare, T., Higgins, C.P., 2021. The Mass Transfer Index (MTI): A semi-empirical approach for quantifying transport of solutes in variably saturated porous media. Journal of Contaminant Hydrology 242, 103842. https://doi.org/10.1016/j.jconhyd.2021.103842

Stults, J.F., Choi, Y.J., Rockwell, C., Schaefer, C.E., Nguyen, D.D., Knappe, D.R.U., Illangasekare, T.H., Higgins, C.P., 2023. Predicting Concentration- and Ionic-Strength-Dependent Air–Water Interfacial Partitioning Parameters of PFASs Using Quantitative Structure–Property Relationships (QSPRs). Environ. Sci. Technol. 57, 5203–5215. https://doi.org/10.1021/acs.est.2c07316

Stults, J.F., Choi, Y.J., Schaefer, C.E., Illangasekare, T.H., Higgins, C.P., 2022. Estimation of Transport Parameters of Perfluoroalkyl Acids (PFAAs) in Unsaturated Porous Media: Critical Experimental and Modeling Improvements. Environ. Sci. Technol. 56, 7963–7975. https://doi.org/10.1021/acs.est.2c00819

Umeh, A.C., Naidu, R., Shilpi, S., Boateng, E.B., Rahman, A., Cousins, I.T., Chadalavada, S., Lamb, D., Bowman, M., 2021. Sorption of PFOS in 114 Well-Characterized Tropical and Temperate Soils: Application of Multivariate and Artificial Neural Network Analyses. Environ. Sci. Technol. 55, 1779–1789. https://doi.org/10.1021/acs.est.0c07202

van Genuchten, M.Th., Wagenet, R.J., 1989. Two-Site/Two-Region Models for Pesticide Transport and Degradation: Theoretical Development and Analytical Solutions. Soil Science Society of America Journal 53, 1303–1310. https://doi.org/10.2136/sssaj1989.03615995005300050001x

Van Glubt, S., Brusseau, M.L., Yan, N., Huang, D., Khan, N., Carroll, K.C., 2021. Column versus batch methods for measuring PFOS and PFOA sorption to geomedia. Environmental Pollution 268, 115917. https://doi.org/10.1016/j.envpol.2020.115917

Wagenmakers, E.-J., Farrell, S., 2004. AIC model selection using Akaike weights. Psychonomic Bulletin & Review 11, 192–196. https://doi.org/10.3758/BF03206482

Wallis, I., Hutson, J., Davis, G., Kookana, R., Rayner, J., Prommer, H., 2022. Model-based identification of vadose zone controls on PFAS mobility under semi-arid climate conditions. Water Research 225, 119096. https://doi.org/10.1016/j.watres.2022.119096

Wang, Y., Khan, N., Huang, D., Carroll, K.C., Brusseau, M.L., 2021. Transport of PFOS in aquifer sediment: Transport behavior and a distributed-sorption model. Science of The Total Environment 779, 146444. https://doi.org/10.1016/j.scitotenv.2021.146444

Wanzek, T., Stults, J.F., Johnson, M.G., Field, J.A., Kleber, M., 2023. Role of Mineral–Organic Interactions in PFAS Retention by AFFF-Impacted Soil. Environ. Sci. Technol. 57, 5231–5242. https://doi.org/10.1021/acs.est.2c08806

Yang, S.-H., Shan, L., Chu, K.-H., 2022. Fate and Transformation of 6:2 Fluorotelomer Sulfonic Acid Affected by Plant, Nutrient, Bioaugmentation, and Soil Microbiome Interactions. Environ. Sci. Technol. 56, 10721–10731. https://doi.org/10.1021/acs.est.2c01867

Zeng, J., Guo, B., 2023. Reduced Accessible Air–Water Interfacial Area Accelerates PFAS Leaching in Heterogeneous Vadose Zones. Geophysical Research Letters 50, e2022GL102655. https://doi.org/10.1029/2022GL102655

Zeng, J., Guo, B., 2021. Multidimensional simulation of PFAS transport and leaching in the vadose zone: Impact of surfactant-induced flow and subsurface heterogeneities. Advances in Water Resources 155, 104015. https://doi.org/10.1016/j.advwatres.2021.104015

Zhang, W., Guo, B., 2024. Anomalous Adsorption of PFAS at the Thin-Water-Film Air-Water Interface in Water-Unsaturated Porous Media. Water Resources Research 60, e2023WR035775. https://doi.org/10.1029/2023WR035775

Zhou, D., Brusseau, M.L., Zhang, Y., Li, S., Wei, W., Sun, H., Zheng, C., 2021. Simulating PFAS adsorption kinetics, adsorption isotherms, and nonideal transport in saturated soil with tempered one-sided stable density (TOSD) based models. Journal of Hazardous Materials 411, 125169. https://doi.org/10.1016/j.jhazmat.2021.125169

Zhuang, L., Coelho, C.R.B., Hassanizadeh, S.M., Genuchten, M.T. van, 2017. Analysis of the Hysteretic Hydraulic Properties of Unsaturated Soil. Vadose Zone Journal 16, vzj2016.11.0115. https://doi.org/10.2136/vzj2016.11.0115

Zhuang, L., Raoof, A., Mahmoodlu, M.G., Biekart, S., De Witte, R., Badi, L., Van Genuchten, M.Th., Lin, K., 2021. Unsaturated flow effects on solute transport in porous media. Journal of Hydrology 598, 126301. https://doi.org/10.1016/j.jhydrol.2021.126301